Available online at www.sciencedirect.com
SCIENCE DIRECT
Thermochimica Acta 438 (2005) 155–163
thermochimica acta
www.elsevier.com/locate/tca

Qualitative study of the evolution of the composition of the gas evolved in the thermal and HY-catalytic oxidative degradation of EVA copolymers

A. Marcilla, A. Gómez-Siurana *, S. Menargues

Dpto. Ingeniería Química, Universidad de Alicante, Apdo. 99, 03080 Alicante, Spain

Received 29 June 2005; received in revised form 19 July 2005; accepted 24 July 2005
Available online 29 September 2005

Abstract

In this work, a study of the evolution with the temperature of the qualitative composition of the gas evolved in the degradation of ethylene-vinyl acetate (EVA) copolymers under air atmosphere has been carried out using on-line analysis by thermogravimetry (TGA) combined with FTIR spectrometry (TGA/FTIR). Three commercial EVA copolymers were selected, and the results obtained in the experiments performed in the presence and in the absence of HY zeolite are compared. The air atmosphere causes significant differences among the thermal and catalytic pyrolysis. The oxidative pyrolysis involves four main decomposition steps, and each of them also involves different types of reactions. In the first stage, the loss of acetoxi groups of the VA units occurs, with formation of acetic acid, but also CO, CO_2 and carbonylic compounds are produced, increasing the formation of these compounds as the VA content of the copolymer decreases. The second and third decomposition steps, which are better distinguished as the VA content of the copolymer increases, correspond to the degradation of the polymeric chain which results from the previous step, and involves cracking reactions, without O_2 consumption, as well as oxidation reactions. Finally, the fourth reaction step corresponds to the slower oxidation of the carbonous residues formed in the previous stages. The presence of the HY zeolite contributes to a decrease of the CO and CO_2 formation, or in other words, to an increase of the reactions without oxygen consumption.

Keywords: EVA copolymers; Oxidative degradation; TGA; FTIR; HY zeolite

1. Introduction

The importance and interest of the study of the possible recycling of ethylene-vinyl acetate (EVA) copolymers wastes by catalytic pyrolysis or by oxidative thermal degradation, in order to obtain useful energetic products or valuable chemicals has been shown previously [1–3]. The study of the oxidative pyrolysis has added interest since it is always present in the earlier stages of the combustion processes, which are important waste disposal alternatives to be considered on many occasions. Moreover, the ability of the combination of thermogravimetric analysis (TGA) and FTIR spectrometry (TGA/FTIR) as a technique for showing the evolution with the time or the temperature of the composition of the gas evolved in pyrolysis processes has also been demonstrated in bibliographies [4–6], and interesting conclusions related to the nature of the chemical reactions involved in the degradation processes can be obtained from the analysis of the changes in the IR absorption bands corresponding to the functional groups or the chemical bonds present in the volatile products evolved from the TGA furnace.

The mechanisms involved in the thermal oxidation of polymers have been studied by several authors [1,7,8]. According to Allen et al. [8], the thermal oxidation of EVA copolymers proceeds by an initial loss of acetic acid, followed by oxidation and breakdown of the main chain. FTIR spectroscopic analysis of the oxidized EVA shows the evidence for deacetylation followed by the concurrent formation of hydroxil/hydroperoxide species, ketone groups, α–β

* Corresponding author. Tel.: +34 965903400x2953; fax: +34 965903826.
E-mail address: Amparo.gomez@ua.es (A. Gómez-Siurana).

0040-6031/$ – see front matter © 2005 Elsevier B.V. All rights reserved.
doi:10.1016/j.tca.2005.07.015

unsaturated carbonyl groups, conjugated dienes, lactones and various substituted vinyl groups. The hydroperoxide evolution follows typical auto-oxidation kinetics forming ketonic species. Moreover, García and Font [1] showed that the pyrolysis and combustion processes of an EVA refuse can be perfectly simulated by two series reactions, the second reaction beginning when the first one has almost finished.

Prior results [9] showed that in the oxidative degradation of EVA with MCM-41, four main reaction steps appear, with and without catalyst, and the presence of the catalyst does not seem to significantly affect the peak temperature of the processes, with the only exception of the second one, which is slightly displaced to lower temperatures in the presence of the catalyst. By analogy with the weight loss and the behaviour observed in the EVA pyrolysis process (i.e., in the presence of inert atmosphere), the first decomposition step was related to the acetate groups' loss [3]. The second and third decomposition steps occurred at very close temperatures and produce overlapped peaks in the derivative of the TGA curves (DTG curves), which cannot always be distinguished, and that were associated to the decomposition of the polymeric chain formed once the acetate groups have been eliminated in the first decomposition step, through reactions with and without oxygen consumption. Finally, the last decomposition step was related to a slow oxidation of non-volatile residues formed in the previous steps.

In the present work, the thermal and catalytic degradation of EVA copolymers under air atmosphere has been studied using TGA/FTIR analysis, in order to confirm the different types of reactions involved. In this way, three commercial EVA copolymers with different vinyl acetate (VA) content and melt flow index (MFI), and a HY zeolite have been selected. HY zeolite has been selected because is a catalyst widely studied for the pyrolysis of polymers, and especially for the pyrolysis of EVA [10,11]. In previous works, we have studied the thermal [6] and HY-catalytic pyrolysis [10,11] of EVA copolymers. In the present work, we focus on the thermal and catalytic oxidative pyrolysis of such copolymers in order to study the influence of the oxidative atmosphere and the presence of the catalyst in the pyrolysis process.

2. Experimental

Table 1 shows the main characteristics (as provided by the supplier) of the three commercial EVA studied and the notation used in this work. HY zeolite was prepared by conventional hydrothermal synthesis as described elsewhere [12] and has a pore size of 7.4 Å, a specific area of 750 m^2/g and a molar ratio SiO_2/Al_2O_3 of 12.

Mixtures of powdered copolymer and catalyst of around 5 mg, with around 10% (w/w) of HY zeolite, were pyrolysed in an air atmosphere (21%, v/v, O_2 and 79%, v/v, air; 99.995% minimum purity) using a TGA Netzsch TG209 and at heating rate of 35 K/min. To ensure the measurement of the actual sample temperature, a calibration of the temperature was performed using the Curie-point transition of standard metals. With this equipment, the accuracy of the measurements of the sample temperature was less than 0.5 K, with a resolution of 0.1 K. The nominal resolution of the mass measurement was 0.1 μg. On the other hand, all the experiments were replicated at least twice to ensure its reproducibility.

The output of the inert gas from the TGA was connected to a Bruker Tensor 27 FTIR spectrometer through a heated line, as described in bibliography [13]. The low volumes in the thermobalance microfurnace, transfer line and gas measurement cell permit low carrier gas flowrates to be used and allow the detection of the gases evolved in the pyrolysis process. In all the experiments, the transfer line and the gas measurement cell were maintained at 473 K, in order to avoid the condensation of the less volatile compounds.

3. Results and discussions

3.1. Analysis of the GS and DTG curves

The selection of the analysis conditions (i.e., the heating rate) is a matter of great importance in order to interpret the results provided by the different analytical techniques. According to Berbenni et al. [14], high heating rates are required to obtain adequate concentration in the FTIR spectrometer coupled with the thermobalance to be correctly detected. Nevertheless, in such conditions, the processes observed by the weight loss analysis are likely to be overlapped. Thus, a type of compromise solution must be adopted in order to enable the objective of the study to be reached. In this case, we focus on the analysis of the FTIR data and, consequently, we have selected a high heating rate (i.e., 35 K/min). In a previous work [9] and focusing on the analysis of the weight loss data, we selected 10 K/min that allowed better representation of the processes in the TGA. In this work, we corroborate and clarify previous results obtained.

Fig. 1 shows the TGA and Gram–Schmidt (GS) curves obtained for the oxidative degradation of the three EVA studied, both in the presence and in the absence of HY zeolite.

Table 1
Characteristics of the three commercial EVA copolymers studied

Commercial name of polymer	VA%	MFI[a] (ASTM D1238)	Hardness (Shore A)	Nomenclature
EVA BASF LUPOLEN U-3510-K	13	4	84	EVA0
EVA EXXON ESCORENE UL-15028-CC	27.5	145	69	EVA1
EVA ESCORENE UL-00728	27.5	7	78	EVA2

[a] MFI: melt flow index (g/10 min).

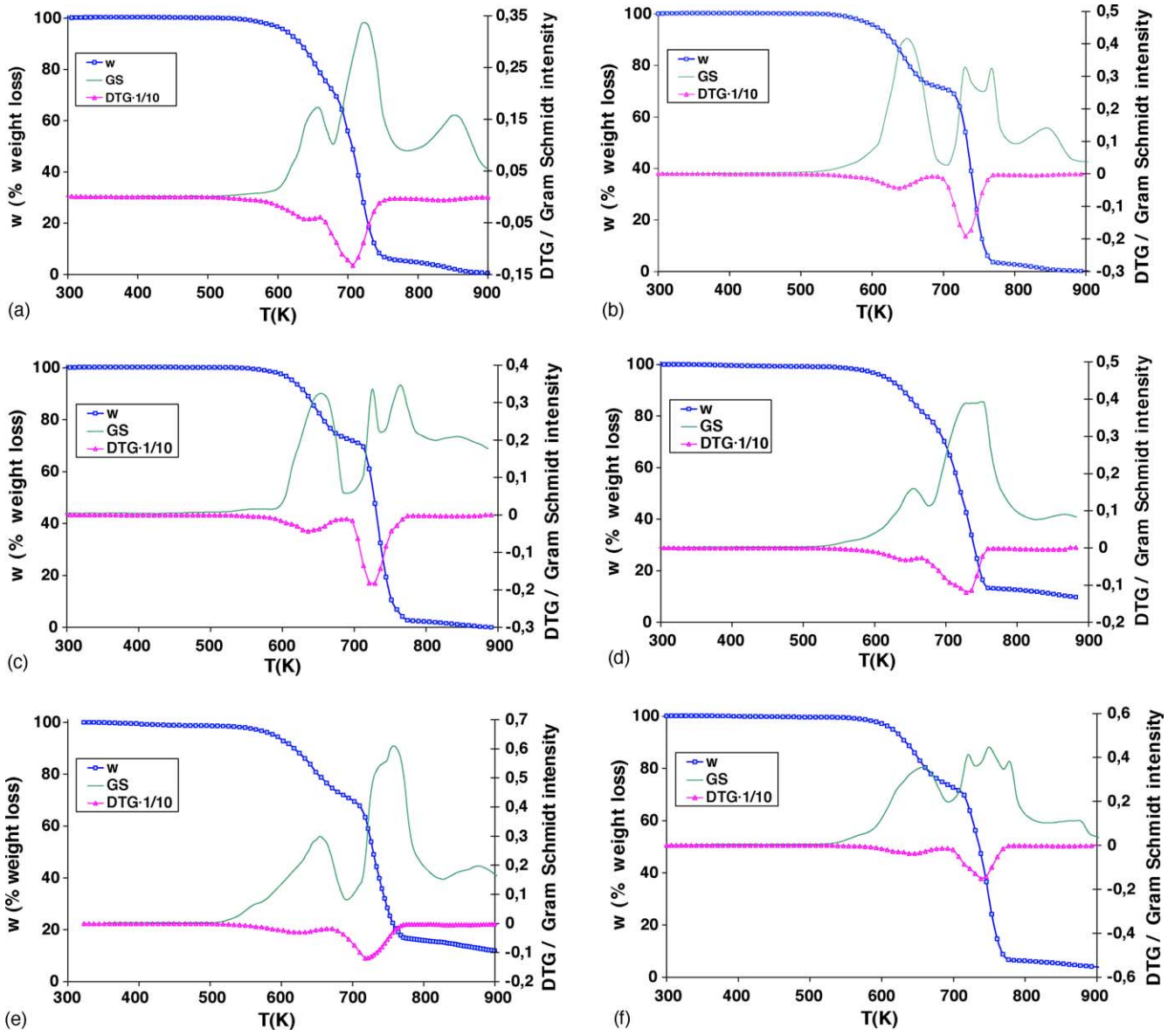

Fig. 1. TGA, DTG and GS curves obtained for the decomposition in air atmosphere of different systems (35 K/min). (a) EVA0, (b) EVA1, (c) EVA2, (d) EVA0 + HY, (e) EVA1 + HY and (f) EVA2 + HY.

The corresponding derivatives of TGA (DTG) curves are also shown. The GS curves reconstruct, based on vector analysis, the acquired FTIR interferograms, allowing the plots of the total evolved gases detected by the spectrometer to be obtained.

Fig. 1(a–f) allows a preliminary comparison between the processes undergone by the polymer in the presence and in the absence of HY zeolite. Fig. 1(a–c) shows the TGA, DTG and GS curves obtained for the thermal pyrolysis of each EVA copolymer studied. As can be seen, the corresponding TGA and DTG curves show the existence of the main stages of EVA decomposition (i.e., firstly loss of acetate groups, afterwards the chain degradation and, finally, the slow oxidation of the less volatile residues). Moreover, the second main peak of the GS curves obtained for EVA1 and EVA2 shows a splitting in two overlapping peaks, reflecting the existence of two different processes involved in the main decomposition step, as has been mentioned in Section 1, and that can be related to different types of reactions, probably corresponding to processes with and without oxygen consumption [9]. However, the lower VA content of EVA0, together with to the experimental conditions used in this work, does not permit a distinction between the former reactions, although they were clearly observed in a previous work [9] from the TGA curves.

With respect to the oxidative pyrolysis carried out in the presence of HY zeolite, for EVA0 and EVA1 (Fig. 1(d and e)), the split of the main degradation step showing the existence of the second and third decomposition step cannot be observed, in spite of the corresponding DTG and GS curves showing a shoulder which must be related to these processes. A

similar shoulder can also be observed in Fig. 1(a), for EVA0. A different situation is shown by EVA2 (Fig. 1(f)), where the overlapping of three different peaks in the GS curve can be observed. In fact, the above-mentioned splitting of the main peak in Fig. 1(b and c) also reveals the existence of more complex processes. Therefore, in this work, the existence of four reaction steps in the catalytic oxidative degradation of EVA previously suggested [9] is corroborated, even at the higher heating rate used in order to optimise the FTIR analysis.

As can be seen in Fig. 1, the presence of HY zeolite contributes to the overlapping between the second and third decomposition steps. This fact may be related to the known catalytic effect of the HY zeolite, decreasing the temperature of the cracking reactions [13], i.e., the reactions without oxygen consumption.

3.2. Analysis of the FTIR spectrograms

In order to obtain information about the evolution with the temperature of the composition of the gas evolved from the TGA furnace, the three-dimensional diagrams (3D diagrams) corresponding to the thermal and catalytic oxidative degradation of EVA have been obtained. These diagrams show the evolution with time (or temperature) of the FTIR spectra corresponding to the products generated in the TGA furnace. Fig. 2 shows, as an example, the 3D diagrams corresponding to the thermal and catalytic oxidative degradation of EVA0. Similar diagrams have been obtained for EVA1 and EVA2. As can be seen, at least three fronts of absorbance bands appear, corresponding to the different reaction steps, being the second one constituted by the overlapping peaks observed in the GS curves of Fig. 1. The obtention of selected FTIR spectra from the 3D diagrams permits the detailed analysis of the absorption bands corresponding to the volatile products generated at each temperature.

Despite the four main decomposition steps previously described, and in good agreement with the behaviour reflected in the GS curve of Fig. 1(f), also discussed above, the 3D diagrams obtained reveal that the oxidative degradation of EVA is a very complex process, and involves a large number of different reactions or steps. As an example, Fig. 3 shows a magnification of the absorbance bands corresponding to the first decomposition step in the 3D diagram obtained for EVA1. As can be seen, this step seems to be more complicated than the TGA and GS curves reflect, and several nearly simultaneous processes occur. As an example, the bands at 2343 and 2299 cm^{-1}, characteristic of CO_2, show two peaks, the first appearing in cycle 102 (corresponding to 854 s) and the second one at the temperature of maximum decomposition rate for the first decomposition step (at

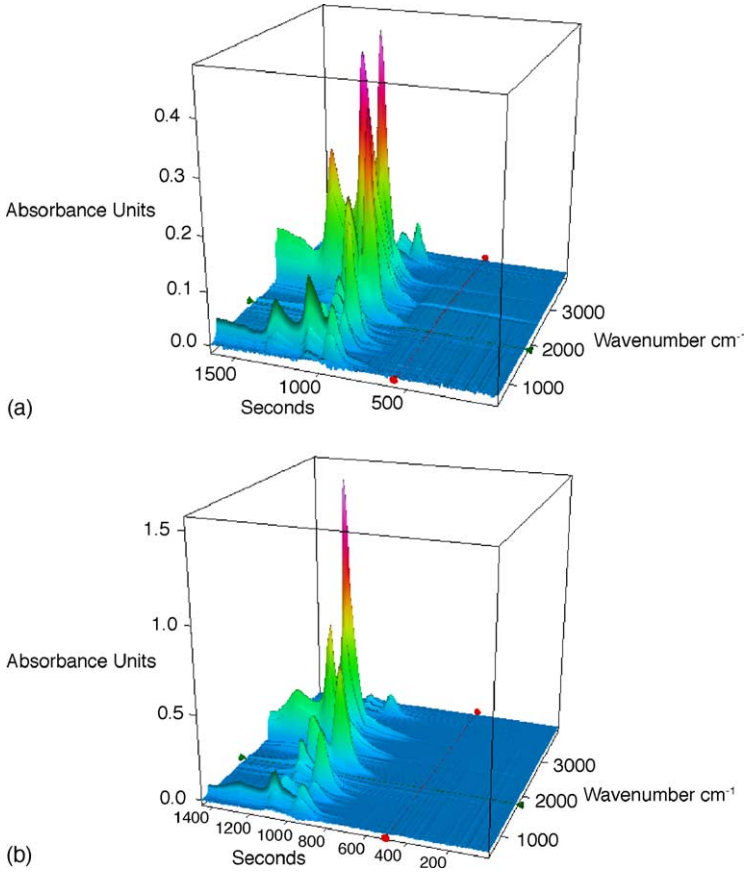

Fig. 2. 3D diagrams for the degradation of EVA0 under air atmosphere at 35 K/min. (a) Thermal process and (b) process carried out in the presence of HY zeolite.

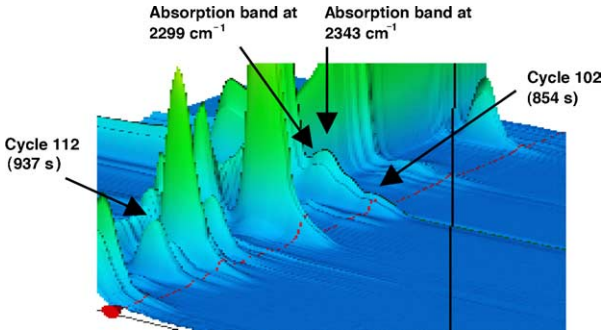

Fig. 3. Magnification of the absorbance bands corresponding to the first decomposition step in the 3D diagram obtained for EVA1.

cycle 112, corresponding to 937 s). 3D diagrams reveal that the compounds showing these preliminary peaks are mainly CO, CO_2 and H_2O. All these compounds are typically generated in oxidation processes, whereas acetic acid and other carbonylic compounds exhibit single peaks, which are those mainly responsible for the peaks corresponding to the first decomposition step.

For the purpose of analyzing the evolution with the temperature of the qualitative composition of the gas evolved in the oxidative degradation process, the FTIR spectra corresponding to the gas evolved at the temperatures of the maxima of GS curves (i.e., to the temperatures of maximum rate of reaction for each decomposition step) have been extracted from the different 3D diagrams. Thus, Fig. 4 shows the FTIR spectra corresponding to the gas evolved in the first decomposition step for the different systems studied. These spectra reveal the major formation of acetic acid (i.e., bands at 3580, 1798, 1381 and 1175 cm^{-1}), CO (bands at 2158 and 2120 cm^{-1}) and CO_2 (bands at 2343 and 2299 cm^{-1}), as in the thermal and catalytic pyrolysis [5,6], and also H_2O (bands at 3562–3593 cm^{-1}) and carbonylic compounds (bands at 1740–1720 cm^{-1}). Despite the resemblance between the composition of the gas evolved in the first step of EVA decomposition in inert and oxidizing atmosphere, which in both cases is mainly composed of acetic acid, in the oxidizing atmosphere a noticeable increase in the CO, CO_2 and H_2O formation has been observed (see Fig. 5), mainly in the EVA0 case, being obviously related to its lower VA content. On the other hand, Fig. 6 shows that the air atmosphere also favours the formation of other oxygenated compounds, different from acetic acid (probably aldehydes, see Table 2), from the EVA0 degradation.

The comparison among the spectra corresponding to the gas evolved in the first step of oxidative decomposition of EVA (Fig. 4) also reveals that the volatile product obtained from the EVA0 sample, in the presence and in the absence of HY zeolite, shows a noticeable increase of the bands

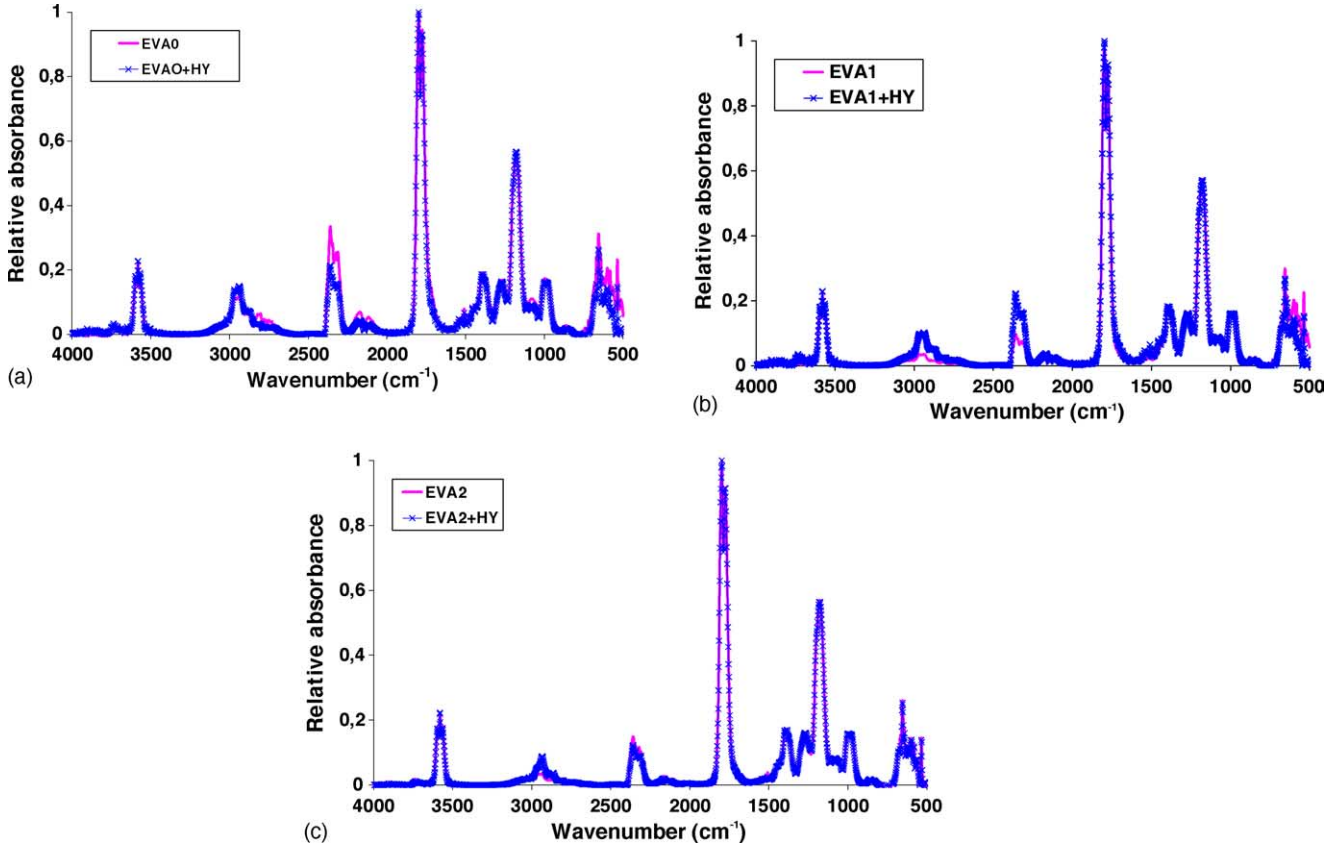

Fig. 4. FTIR spectra corresponding to the gas evolved at the maximum decomposition rate in the first step of the oxidative degradation of EVA and EVA + HY. (a) EVA0, (b) EVA1 and (c) EVA2.

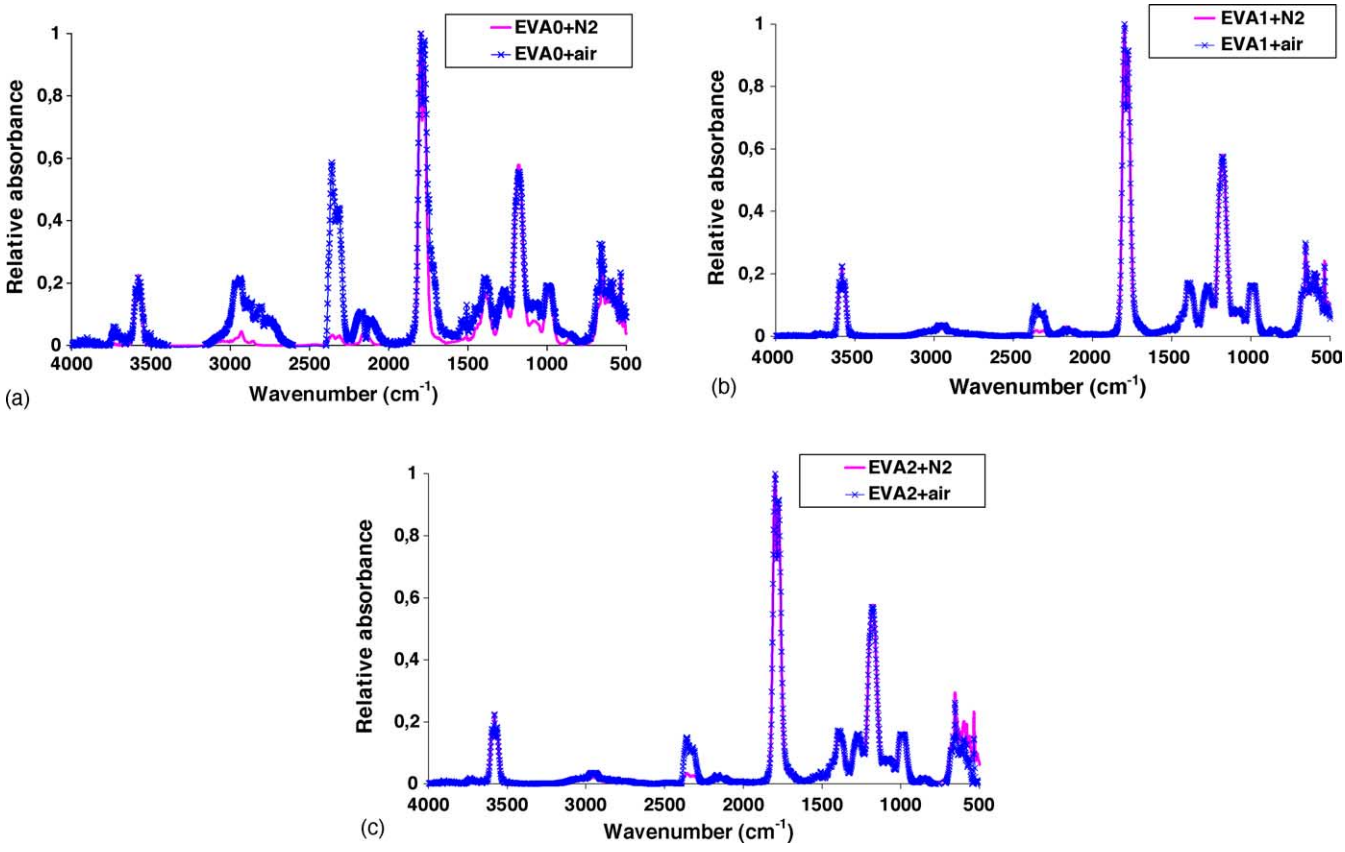

Fig. 5. Comparison between the FTIR spectra corresponding to the gas evolved at the maximum decomposition rate in the first step of the degradation of EVA carried out in air and in N_2 atmospheres. (a) EVA0, (b) EVA1 and (c) EVA2.

appearing in the zone 2964–2856 cm^{-1}, corresponding to stretching vibrations of alkanes. This fact can be related to the above-mentioned behaviour of EVA0, favouring the CO, CO_2 and carbonylic compounds formation, and may be related to the alkyl groups linked, in different environments, to the C=O group. Another possible explanation is related to the CH_4 formation which, according to bibliographies [4–6], accompanies the secondary processes yielding CO and CO_2 in the

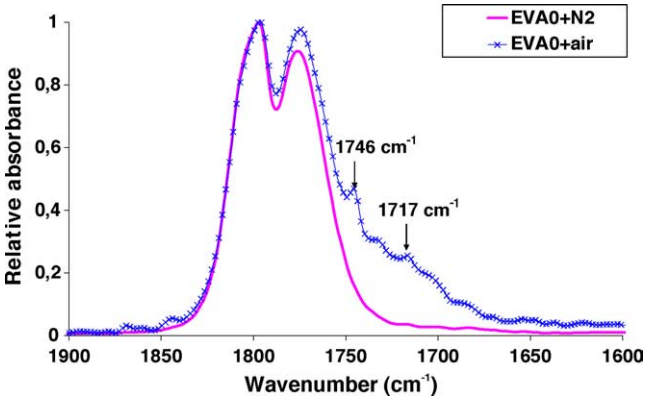

Fig. 6. Magnification of the region near to 1774 cm^{-1} in the FTIR spectra corresponding to the gas evolved at the maximum decomposition rate in the first step of the degradation of EVA0 carried out in air and in N_2 atmospheres.

Table 2
Assignments of the IR bands to vibrational modes of atomic groups

Wavenumber (cm^{-1})	Vibrational mode
First stage of decomposition	
3562–3593	Free –OH
2747	Aldehydic C—H stretching
2299, 2343	CO_2
2158, 2120	CO
1798	C=O stretching CH_3COOH
1740–1720	Aliphatic aldehydes
1396, 1369	Stretching C—O—H
1390	Aldehydic C—H stretching
1267, 1175	Stretching C—O in CH_3COOH
716–642	Out-of-plane bending of –OH
Second and third stage of decomposition	
3709, 1514	H_2O
3100–3000, 1600–1585, 1300–1100, 909–650	Mononuclear aromatic hydrocarbons
3015	Olefinic stretching
2964	Asymmetrical stretching of $–CH_3$
2926	Asymmetrical stretching of $–CH_2–$
2862	Symmetrical stretching of $–CH_3$
2856	Symmetrical stretching of $–CH_2–$
2299, 2343	CO_2
2158, 2120	CO
1514	H_2O
1375	Symmetrical bending of $–CH_3$
1450	Asymmetrical bending of $–CH_3$
1465	Scissoring of $–CH_2–$

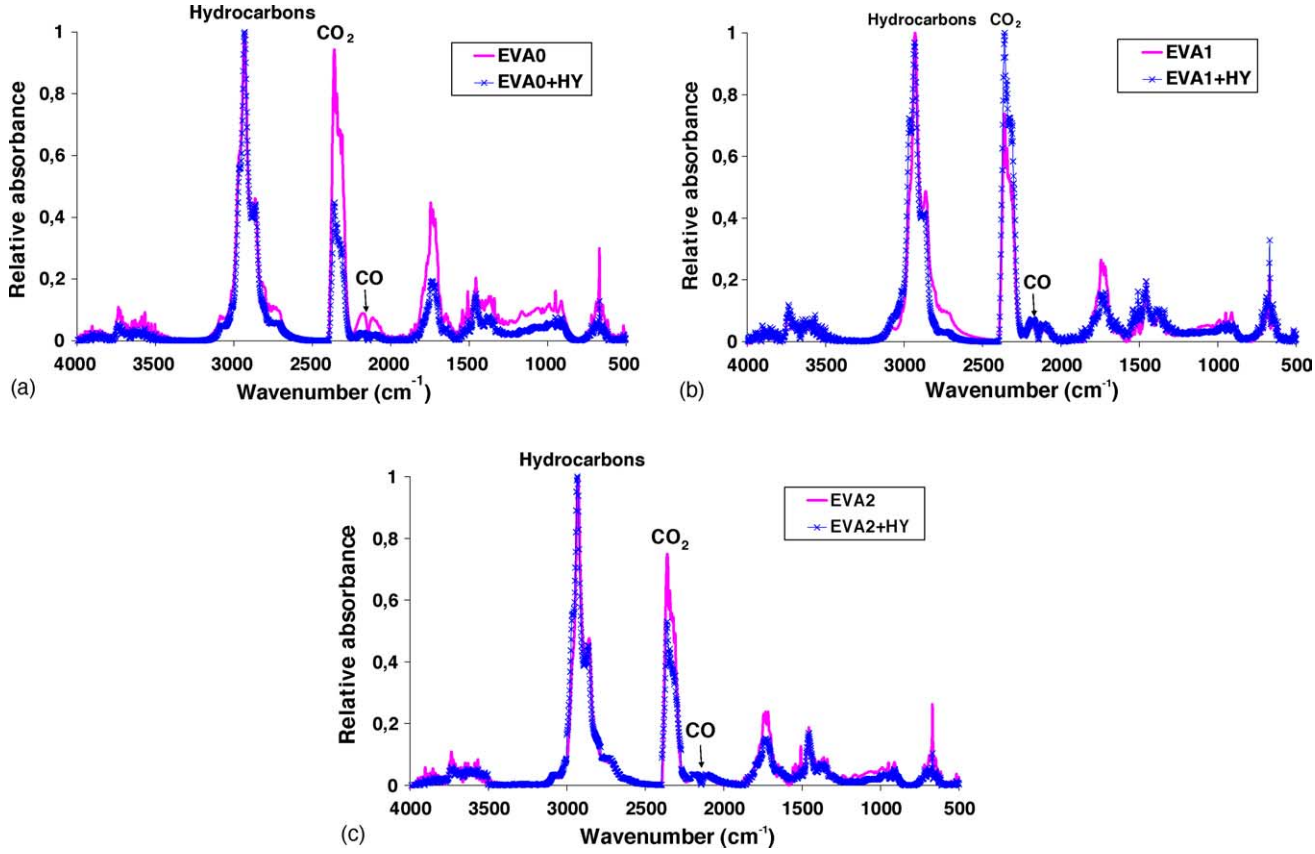

Fig. 7. FTIR spectra corresponding to the gas evolved at the maximum decomposition rate in the main step (second + third) of the oxidative degradation of EVA and EVA + HY. (a) EVA0, (b) EVA1 and (c) EVA2.

EVA pyrolysis process. In this way, the results shown in Fig. 5 also show for EVA0 a noticeable increase of the bands in the region 2964–2856 cm^{-1}, together with the increase of the bands of CO and CO_2.

Fig. 7 shows the FTIR spectra corresponding to the gas evolved in the second and third decomposition steps of oxidative EVA decomposition. As has been stated previously, a clear differentiation between them cannot always be made and, in any case, the corresponding FTIR spectra are very similar, as a consequence of the fact that the processes involved are nearly simultaneous. However, Fig. 7 shows the presence of IR absorption bands corresponding to the decomposition products originated in different reactions. The analysis of the IR spectra of Fig. 7, together the assignment of the IR bands to vibrational modes of atomic groups (Table 2), permit to analyze the qualitative composition of the gas evolved once the acetate groups have been eliminated. These spectra are very similar to those corresponding to the main decomposition step of the thermal and catalytic EVA pyrolysis, which have been already described in bibliographies [5,6,11], and the bands assigned to a "hydrocarbons mixture" reflect the existence of 1-alkenes and alkanes mixture, with the presence of other minor compounds such as mononuclear aromatic compounds. On the other hand, bands corresponding to CO and CO_2 and H_2O also appear, reflecting the existence of oxidation processes. This behaviour suggests that, in these steps, despite the air atmosphere which permits oxidation reactions (yielding CO, CO_2 and H_2O), some cracking (without O_2) of the polymeric chain, yielding a hydrocarbon mixture, also occurs simultaneously. The overlapping between the second and third degradation events makes it difficult to distinguish among the compounds evolved in each one. The corresponding 3D diagrams also show this overlapping, and reflect the existence of very similar FTIR spectra at the temperature of maximum reaction rate for each degradation step. However, according to previous results [9], both steps involve cracking and oxidation reactions, despite the contribution of the cracking reactions to the second decomposition step seems to be higher than the contribution of the oxidation reactions, whereas the third decomposition step shows the opposite tendency.

According to Fig. 7, the effect of the catalyst on the relative intensity of the absorption bands corresponding to CO and CO_2 in the gas obtained in the second + third oxidative decomposition step of EVA decreases as the amount of VA in the polymer increases. Additionally, in the case of EVA0 and EVA2 this intensity decreases in the presence of HY zeolite, indicating that the presence of this catalyst enhances the cracking processes which occur simultaneously to the oxidation or, in other words, decreases the relative importance of the oxidation reactions. In the EVA1 case, a different trend has been observed, and the relative absorbance of the

Table 3
Ratio between the relative absorbance obtained for bands corresponding to CO_2 in the thermal and catalytic oxidative degradation processes

	First step	Second + third steps	Fourth step
EVA0/EVA0 + HY	1.69	2.11	1.04
EVA1/EVA1 + HY	0.35	0.74	0.98
EVA2/EVA2 + HY	1.23	1.42	1.09

Values corresponding to the main band (at around 2350 cm^{-1}) in the gas evolved at the maximum decomposition rate of the first and second + third decomposition step and for the band at around 2300 cm^{-1} for the fourth step are shown.

CO and CO_2 bands are higher in the catalytic process. This fact may be related to the high MFI of EVA1 (see Table 1) which indicates that the polymer–catalyst and oxygen mixing and diffusion processes may be very different, and noticeably favoured, for this copolymer as compared to EVA0 and EVA2. Similar behaviour can be observed for the first decomposition step (Fig. 4) but, in this case, the lower extent of the oxidation processes related to the HY presence is much lower. To illustrate this behaviour, Table 3 shows the ratio between the relative absorbance of the more intense band for CO_2 (at around 2350 cm^{-1}) in the thermal and catalytic processes, obtained for each decomposition step. As can be seen, the values obtained for EVA0 and EVA2 are greater than 1, indicating higher generation of CO_2 in the thermal processes, and the values are higher for the first than for the second + third decomposition steps.

Finally, the spectrum corresponding to the gas evolved in the fourth decomposition step (Fig. 8) is similar to that obtained in the previous step, but showing a noticeable decrease of the bands corresponding to vibrational modes of hydrocarbons. In effect, whereas the more intense band in the spectra of Fig. 7 appears at around 2926 cm^{-1}, corresponding to the asymmetrical stretching of $–CH_2–$, the more intense band in the spectra of Fig. 8 is at around 2343 cm^{-1}, and corresponds to CO_2. Thus, this behaviour reflects that, in the last decomposition step, the reactions without oxygen consumption decrease compared with the oxidation processes. In this step, the decrease of the CO and CO_2 generation in the oxidative pyrolysis of EVA0 and EVA2 carried out in the presence of HY zeolite is also observed (see Table 3). In this case, the main band of CO_2 is the main band of the spectra, and thus, the corresponding relative absorbance is 1. Therefore, the following more intense band (at around 2300 cm^{-1}) has been selected to carry out the comparison between CO and CO_2 formation in the thermal and catalytic processes.

The above-mentioned behaviour gives rise to the conclusion that the following reaction steps occur in the oxidative degradation of EVA:

First step: Degradation of the units of the polymeric chain coming from the VA monomers with formation of acetic

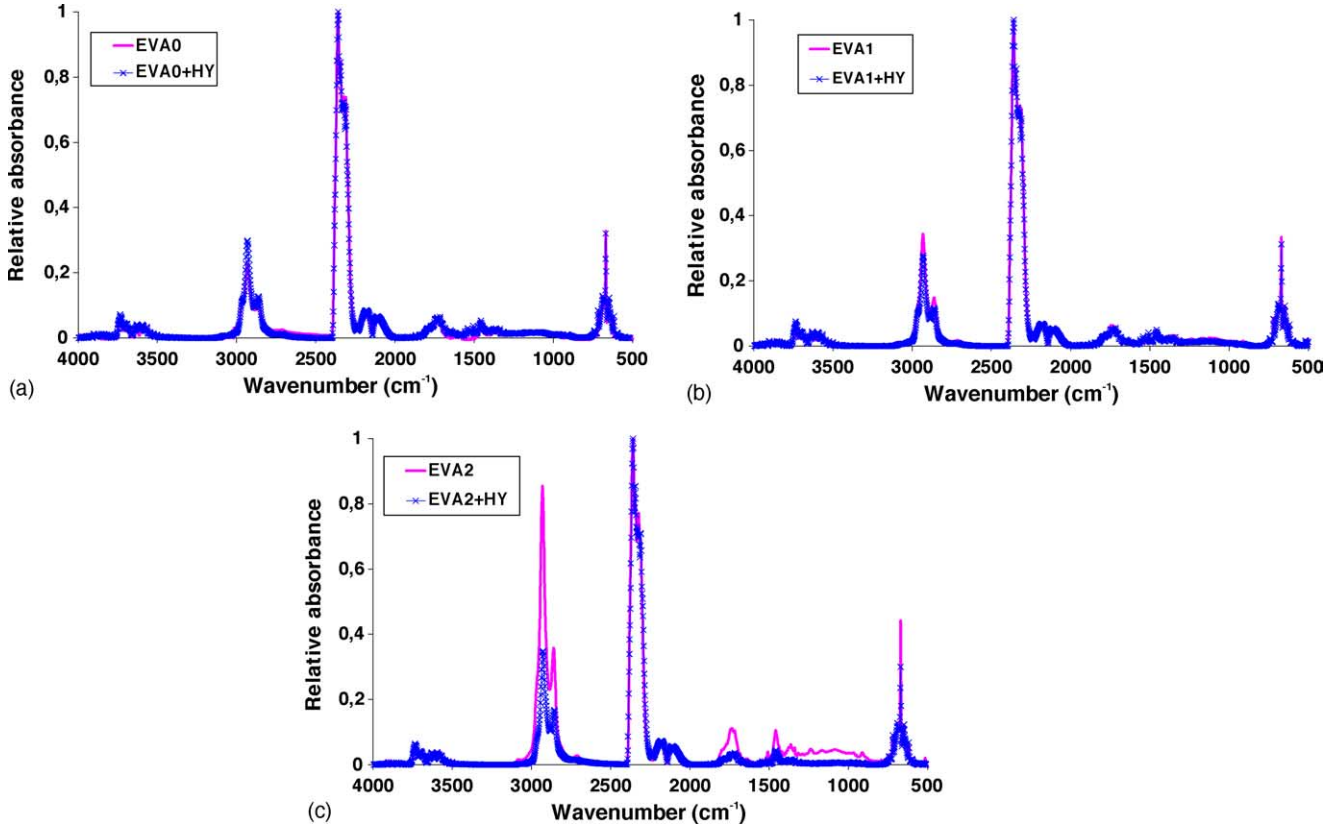

Fig. 8. FTIR spectra corresponding to the gas evolved at the maximum decomposition rate in the last step of the oxidative degradation of EVA and EVA + HY. (a) EVA0, (b) EVA1 and (c) EVA2.

acid, CO, CO_2, H_2O and carbonylic compounds. The formation of the CO, CO_2, H_2O and carbonylic species increases as the VA content of the copolymer decreases.

Second and third steps: Involve at least two types of processes, reactions without O_2 consumption and oxidation processes yielding CO, CO_2 and H_2O. The reactions without O_2 consumption may be similar to that involved in the second step of EVA pyrolysis and, according to Marcilla et al. [2,6] pass through different processes for the decomposition of the ethylene and VA domains. According to previous results [9], the contribution of the cracking reactions to the second decomposition step is higher than the contribution of the oxidation reactions, whereas the third decomposition step shows the opposite tendency.

Fourth step: Oxidation of the less volatile residues formed in the previous steps.

4. Conclusions

In this work, a qualitative study of the evolution with the temperature of the gas evolved in the oxidative degradation of EVA copolymers has been carried out. The results obtained show the existence of a complex process which involves four main decomposition steps, each of them also involving different types of reactions. The differences between the second and third decomposition steps are enhanced for the EVA with low VA content. In the first degradation stage, the loss of acetoxi groups of the VA units occurs, with the major formation of acetic acid, CO and CO_2, and also other carbonylic compounds. The second and third decomposition steps correspond to the degradation of the polymeric chain which results from the previous step and involves both reactions without O_2 consumption, and oxidation reactions. Finally, the fourth reaction step corresponds to the slower oxidation of the carbonous residues formed in the previous stages. The comparison between the results obtained in the absence of and in the presence of HY zeolite suggests that the solid acid catalyst enhances the cracking processes which occur simultaneously to the oxidation and, consequently, reduces the CO and CO_2 content in the gas evolved.

Acknowledgements

Financial support for this investigation has been provided by the Spanish “Comisión de Investigación Científica y Tecnológica” de la Secretaría de Estado de Educación, Universidades, Investigación y Desarrollo and the European Community (FEDER refunds) (CICYT CTQ2004-02187) and by the Generalitat Valenciana (project GRUPOS03/159).

References

[1] A.N. García, R. Font, Fuel 83 (2004) 1165–1173.
[2] A. Marcilla, A. Gómez, S. Menargues, J. Anal. Appl. Pyrol. 68–69 (2003) 507–526.
[3] A. Marcilla, A. Gómez, S. Menargues, R. Ruiz, Polym. Degrad. Stab. 88 (2005) 456–460.
[4] B.J. McGrattan, Appl. Spectr. 48 (12) (1993) 1472–1476.
[5] A. Marcilla, A. Gómez, S. Menargues, Polym. Degrad. Stab. 89 (2005) 145–152.
[6] A. Marcilla, A. Gómez, S. Menargues, J. Anal. Appl. Pyrol. 74 (2005) 224–230.
[7] F. Gugumus, Polym. Degrad. Stab. 53 (1996) 161–187.
[8] N.S. Allen, M. Edge, M. Rodrigues, C.M. Liauw, E. Fontan, Polym. Degrad. Stab. 71 (2001) 1–14.
[9] A. Marcilla, A. Gómez-Siurana, S. Menargues, R. Ruiz-Femenía, J.C. García-Quesada, Oxidative degradation of PE and EVA copolymers in the presence of MCM-41, J. Anal. Appl. Pyrol., submitted for publication.
[10] A. Marcilla, A. Gómez, S. Menargues, J. García-Martínez, D. Cazorla-Amorós, J. Anal. Appl. Pyrol. 68–69 (2003) 495–506.
[11] A. Marcilla, A. Gómez, S. Menargues, Polym. Degrad. Stab. 89 (2005) 454–460.
[12] J. García-Martínez, Ph.D. Thesis, Universidad de Alicante, 2000.
[13] J. Blazek, P. Buryan, D. Grouset, Y. Soudais, V. Tekac, Entropia 235–236 (2001) 6–11.
[14] V. Berbenni, A. Marini, G. Bruni, T. Zerlia, Thermochim. Acta 258 (1995) 125–133.